HYPERFINE-STRUCTURE IN THE 6SNH (1 = 5) RYDBERG SERIES OF BARIUM

Vassen, W.; Vanderveldt, T.; Westra, C.; Bente, E.; Hogervorst, W.

published in
Journal of the Optical Society of America. B: Optical Physics
1989

DOI (link to publisher)
10.1364/JOSAB.6.001473

document version
Publisher's PDF, also known as Version of record

Hyperfine structure in the $6snh$ ($l = 5$) Rydberg series of barium

Wim Vassen, Tony v.d. Veldt, Carel Westra, Erwin Bente, and Wim Hogervorst

Faculteit Natuurkunde en Sterrenkunde, Vrije Universiteit, De Boelelaan 1081, 1081 HV Amsterdam, The Netherlands

Received January 17, 1989; accepted May 1, 1989

The hyperfine structure in the odd-parity $6snh$ ($9 \leq n \leq 40$) Rydberg series of barium has been investigated, using a single cw ring dye laser and a beam of neutral atoms in the metastable $5d^2\,{}^1G_4$ state. Owing to small fine-structure splitting, this hyperfine structure is dominated by the Fermi contact interaction of the $6s$ electron already at $n = 12$. The hyperfine-structure analysis results in a determination of the complete fine structure of the $6snh$ series as well as in values for the singlet–triplet mixing in the $6snh$ $J = 5$ states. The $6snh$ series turn out to be perturbed by levels of the $5d4f$ configuration; $J = 4$ and $J = 5$ levels of this configuration have been observed. The Rydberg series perturbations are analyzed, using multichannel quantum-defect theory in the shifted R-matrix formalism. Far from the $5d4f$ perturbers, the $6snh$ configuration is almost purely jj coupled.

1. INTRODUCTION

Laser spectroscopy of the alkaline earth elements calcium, strontium, and barium has produced a wealth of data on the interaction of regular (bound) Rydberg series with levels of doubly excited configurations.[1,2] In the case of barium the Rydberg series $6snl$ with orbital angular momentum $l < 4$ are heavily perturbed by levels of the $5dml'$ ($l' = 0$–3) and $6p^2$ configurations. These perturbations generally affect many members of the series and result in deviations in the otherwise regular behavior of quantum defect, lifetime, isotope shift, and hyperfine structure. Multichannel quantum defect theory (MQDT) may be used to describe and interpret these data.[1,3]

For higher-l Rydberg series, interactions with doubly excited states are expected to become less important because of the l dependence of the radial integrals, which determine the configuration interaction.[4] This should result in a more regular behavior of the physical observables along the series. In barium the $6sng$ ($l = 4$) Rydberg series are the first with a nonpenetrating Rydberg electron and appeared to have only weak interaction with perturbers. Careful inspection of these series in cw dye-laser experiments, however, showed that, although perturbations by members of the $5d6d$ and $5d7d$ configurations are more localized than perturbations of lower-l Rydberg series, the $6sng$ fine structure behaves irregularly all over the series.[5,6] This has prevented the extraction of parameters of the $6sng$ configuration such as the Slater exchange integral $G^4(6s, ng)$ and the fine-structure constant ξ_{ng}. However, from MQDT analyses of the $6sng$ $J = 3, 4, 5$ series it was concluded that the $6sng$ close-coupling channels are jj rather than LS coupled. To our knowledge, this was not observed before in Rydberg series of the alkaline earth elements.

The $6snh$ series ($J = 4, 5, 6$) will be weakly perturbed by levels of the doubly excited $5d4f$ configuration. Levels of the $5d4f$ configuration with $J = 1, 2$ have been observed by Armstrong *et al.*[7] From these data the complete $5d4f$ configuration is predicted to be located between the $n = 6$ and $n = 10$ levels of the $6snh$ Rydberg series. These expectations were corroborated in a previous experiment on the two $6snh$ $J = 5$ series for ^{138}Ba.[6] The interaction of the $6snh$ series with the $5d4f$ configuration is also of interest for the analysis of $5dnf$ $J = 4, 5$ autoionizing Rydberg series also observed recently in our laboratory. These high-angular-momentum $5dnf$ series show small autoionization linewidths.[8] A MQDT analysis of the perturbed $6snh$ series may in principle be extrapolated into the autoionization regime above the $6s$ ionization limit.

In this paper we report the single-step excitation of the $6snh$ ($n \geq 7$) Rydberg series of barium from the metastable $5d^2\,{}^1G_4$ level, located 24 696.278 cm^{-1} above the $6s^2\,{}^1S_0$ ground state.[6] Signals of all stable isotopes, including ^{130}Ba and ^{132}Ba (natural abundancy 0.1%), were observed by using cw laser excitation. Measurements on the level energies and isotope shifts of even isotopes for $n \geq 10$, $J = 5$ were reported previously.[6] Here we present similar results for $n = 7, 8, 9$ and $5d4f$ perturbers as well as on hyperfine-structure measurements for the odd isotopes ^{137}Ba and ^{135}Ba (natural abundances 11% and 7%, respectively) for $n = 9$–40. The hyperfine structure dominates the fine structure and may be used to extract the composition of the $6snh$ $J = 5$ fine-structure states in terms of singlet–triplet mixing. Also, the $6snh$ $J = 4, 6$ level energies are deduced from the off-diagonal terms in the hyperfine-structure matrix. The fine structure of the perturbed $J = 4, 5, 6$ series is parameterized with MQDT models.

2. EXPERIMENT

Thus far high-l Rydberg series in the alkaline earth elements have not been studied in detail. This is a consequence of the difficulty of populating high-l states from the $l = 0$ ground state. In barium, however, several states of the $5d^2$ configuration are metastable.[9,10] In our cw laser-atomic-beam experiment we used the recently located metastable $5d^2\,{}^1G_4$ state at 24 696 cm^{-1}.[6] From this state the excitation of $6snh$ (and $6snf$) levels is possible owing to configuration mixing in

0740-3224/89/081473-08$02.00

either the upper or the lower state. The $5d^2\,{}^1G_4$ state is populated by collisions in a cloud of slow electrons surrounding a heating filament. This filament was positioned 1 mm in front of a hole in the barium-filled tantalum oven. The collimated barium beam, with a fraction of $\sim 10^{-4}$ in the metastable $5d^2\,{}^1G_4$ state, was intersected perpendicularly by 200-mW light from a Spectra-Physics 380D frequency-stabilized ring dye laser operating with the dye Rhodamine 6G, Rhodamine B, or DCM. The Rydberg atoms were ionized and the detached electrons counted with an electron multiplier. For $n > 20$ we used the field ionization technique to detect the Rydberg atoms: they were ionized a few millimeters downstream from the interaction region in a weak electric field inside a small capacitor. The low-n Rydberg atoms were detected directly in the interaction region; the ionization mechanism in this case is less clear, as we applied only weak fields (1 V/cm) to collect the electrons in the electron multiplier (higher fields resulted in Stark shifts and splittings owing to the large polarizability of the $6snh$ levels). We guess that the primary ionization mechanism is the absorption of blackbody photons. This process is estimated to have a rate of 5000 $\sec^{-1}$ (independent of n).[11] The signal of the electron multiplier was stored on a PDP11 computer, which also controlled the scanning of the laser. Spectra were calibrated by using a 150-MHz length-stabilized étalon. Its transmission peaks were also stored on the computer. More details of the experimental setup can be found elsewhere.[6] The recorded spectra showed a noise level of approximately 100 counts per second; hyperfine signals showed a counting rate of a few thousands per second. The linewidth observed was ~6 MHz FWHM.

Typical excitation spectra $5d^2\,{}^1G_4 \rightarrow 6snh$ are shown in Figs. 1(a) and 1(b) for $n = 12$ and $n = 25$, respectively. In both spectra characteristic groups of lines are apparent. First, for each fine-structure component three peaks belonging to the even isotopes 138, 134, and 136 may be observed (natural abundances 72%, 2%, and 7%). The hyperfine structure (odd isotopes) is divided into two groups of lines on both sides of the even isotopes. This grouping reflects the small hyperfine structure of the $5d^2\,{}^1G_4$ ground state (~0.5 GHz) and the dominant hyperfine structure (~8 GHz) of the $6snh$ levels. In Fig. 1(b) these two groups are labeled with the value of total angular momentum F_c of the Ba^+ core: $\mathbf{F}_c = \mathbf{I} + \mathbf{j}_{6s}$ (nuclear spin $I = 3/2$; $j_{6s} = 1/2$ is the angular momentum of the core electron). They are separated by the ground-state splitting in the Ba^+ ion determined by the $6s$ electron only (hyperfine-structure splitting $2a_c = 8037.74$ MHz for ^{137}Ba). Within each group a further splitting occurs because of the coupling of F_c with the angular momentum of the nh electron: six components for $F_c = 1$ and ten for $F_c = 2$ for each odd isotope. This splitting is determined by the relative position of the four fine-structure components and by the $6snh$ $J = 5$ singlet–triplet mixing. A similar grouping was observed earlier[5] in the $6sng$ Rydberg series in barium for $n > 24$ and is manifest in the $6snh$ series at $n = 12$.

To determine total angular-momentum quantum numbers for the observed transitions we used the recently determined hyperfine structure of the $5d^2\,{}^1G_4$ level,[6,10] the relative abundances of the two odd isotopes, their ion ground-state hyperfine splitting, and the signal strength in the peaks; the $\Delta F = +1$ transitions are usually strong owing to the strong $^1G_4 \rightarrow {}^1H_5$ excitation. Some peaks could not be assigned *a priori* but were identified at a later stage of the analysis. In addition to the grouping determined by F_c we noted that most hyperfine levels appear in pairs. This is illustrated more clearly in Fig. 2, where we plot the hyperfine structure of the $6snh$ configuration as a function of n (n = 9–30) after elimination of the ground-state hyperfine splitting. These pairs have already been observed for $n = 12$. For $n >$ 20 in several cases the levels of such a pair could no longer be resolved. For each pair the total angular momentum is the result of the coupling of F_c with the orbital angular momentum $l = 5$ of the Rydberg electron, giving a new quantum number F_l: $\mathbf{F}_l = \mathbf{F}_c + \mathbf{l}$. For $F_c = 1$ this gives $F_l = 4, 5, 6$, and for $F_c = 2$ $F_l = 3, 4, 5, 6, 7$. Finally, each F_l couples with the spin of the Rydberg electron to give the total angular momentum F ($F = F_l \pm 1/2$), and the total coupling scheme obviously is $\{[(j_{6s}I)F_c l]F_l s\}F$.

Apart from the hyperfine structure some fine-structure levels, not observed before, have also been identified. For n = 8–14 we excited, in addition to the $6snh$ $J = 5$, the $6snh$ $J =$ 4 levels. At $n = 8, 9, 10$ the $J = 4$ signal strength was approximately equal to the two $J = 5$ signals, but for $n > 10$ its intensity dropped rapidly to the level of intensity of hyperfine-structure components [see Fig. 1(a)]; for $n > 14$ J = 4 could no longer be detected. Excitation of $6snh$ $J = 4$ from $5d^2\,{}^1G_4$ is attributed solely to a $5d4f$ admixture in the wave function of the Rydberg state. For $n = 10$ the assignment of one of the two earlier assigned $6s10h$ $J = 5$ levels has to be changed to $6s10h$ $J = 4$.[6] The assignment of J values to the even isotope peaks is confirmed for $n > 8$ by the hyperfine-structure analysis presented in Section 3 and deduced for $n = 8$ from Stark-effect measurements. At 1 kV/cm, owing to the quadratic Stark effect, the three $n = 8$ fine-structure levels split into five and six m components for the J = 4 and $J = 5$ states, respectively. The intensities for $n < 9$ were too weak for hyperfine structure to be measured. At n = 7 only one fine-structure component, most likely $J = 5$, could be observed. These results are included in Tables 1 and 2.

The $5d4f$ perturbers themselves were located in a pulsed dye-laser experiment (see Table 3). Detection in this case was performed on the (green) $5d4f \rightarrow 5d^2\,{}^3F$ fluorescence by using a photomultiplier. The J values of the observed $5d4f$ levels are deduced from extrapolation of data on the $5dnf$ series above the first ionization limit (n = 5–50) recently studied in our laboratory.[8]

3. ANALYSIS

A. Hyperfine Structure

Generally we observed 10–13 of 16 hyperfine components for each odd isotope. The data for ^{135}Ba were not analyzed further, the only difference from ^{137}Ba being the value of the Fermi contact parameter a_c. To analyze the hyperfine structure of the $6snh$ configuration we assume that the only hyperfine interaction of importance is the Fermi contact interaction of the $6s$ electron:

$$H_{\mathrm{hfs}} = a_c \mathbf{I} \cdot \mathbf{s}, \qquad a_c = 4018.87 \text{ MHz } (^{137}\mathrm{Ba}). \tag{1}$$

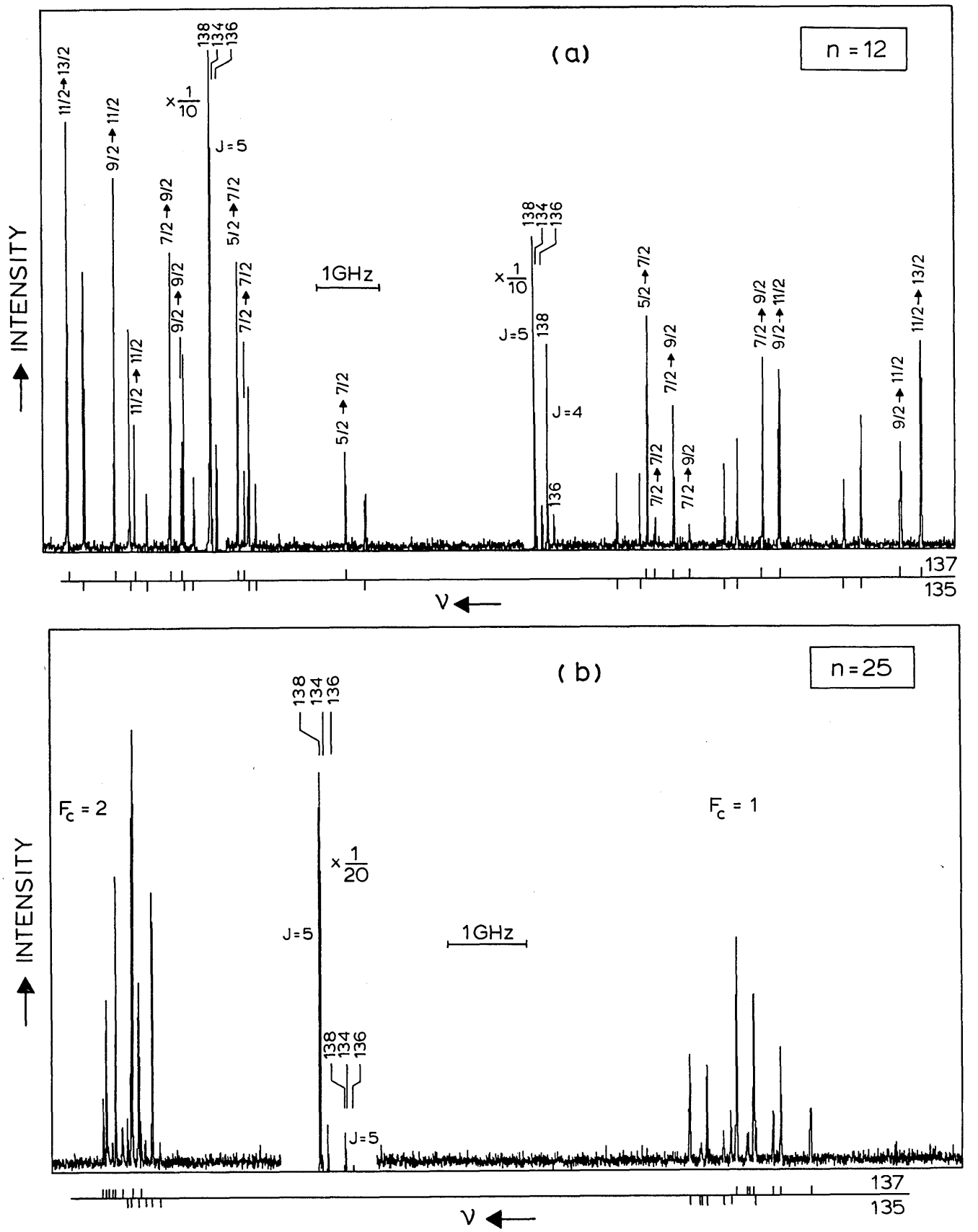

Fig. 1. Excitation spectra $5d^2\,{}^1G_4 \rightarrow 6snh$ for $n = 12$ [(a), $\lambda = 603$ nm] and $n = 25$ [(b), $\lambda = 583$ nm]. The assignment of the hyperfine quantum numbers of ground and excited states is given for ^{137}Ba in (a). The hyperfine peaks in (b) are labeled with the angular momentum F_c of the ion core.

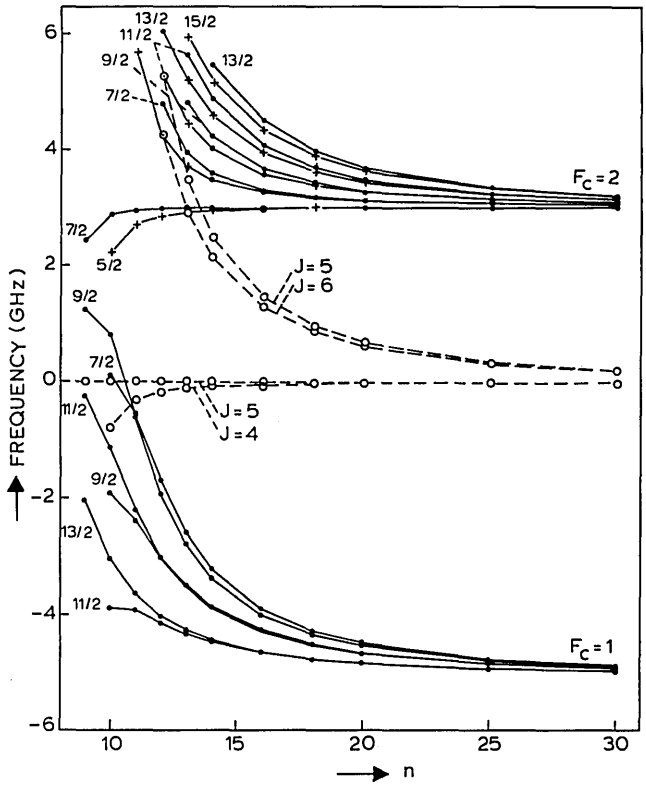

Fig. 2. Fine and hyperfine structure of the 6*snh* configuration as a function of n relative to the ^{138}Ba $5d^2\,{}^1G_4 \rightarrow 6snh\,{}^3H_5$ transition: o, fine-structure (^{138}Ba) levels; ●, hyperfine-structure (^{137}Ba) levels, observed; +, hyperfine-structure (^{137}Ba) levels, deduced from diagonalization (Subsection 3.A).

Contributions of the *nh* electron are ignored, an assumption warranted by the negligible contribution of this electron to the electron density at the nucleus.

The hyperfine structure depends on the positions of the four fine-structure components and their wave functions. Following earlier analyses on 6*snl* Rydberg series,[5] we take as a zero-order basis the fine-structure wave functions

$$
\begin{aligned}
|^1H_5\rangle &= \alpha|^1H_5\rangle_{SL} + \beta|^3H_5\rangle_{SL},\\
|^3H_4\rangle &= |^3H_4\rangle_{SL},\\
|^3H_5\rangle &= \alpha|^3H_5\rangle_{SL} - \beta|^1H_5\rangle_{SL},\\
|^3H_6\rangle &= |^3H_6\rangle_{SL}.
\end{aligned}
\tag{2}
$$

When these expressions (with $\alpha > 0$ the leading coefficient) are used, the contributions of the $5d4f$ configuration in the wave functions, which are small anyhow, are neglected. The terms labeled *SL* are pure *SL*-coupled wave functions. In this SL-coupled basis each of the 16 possible matrix elements $\langle 6snh\ SLIJF|H_{hfs}|6snh\ S'LIJ'F\rangle$ may be evaluated, using angular-momentum algebra. Each basis function of Eqs. (2) has a zero-order energy eigenvalue, which is known from the even isotope spectra for the two $J = 5$ ($n > 8$) and the $J = 4$ ($8 < n < 13$) states. The remaining unknown ($J = 4, 6$) zero-order energies are used as parameters together with β [$\alpha = (1 - \beta^2)^{1/2}$] in a fit to the experimentally observed hyperfine spectrum. A fourth parameter is used to account for the shift of the ^{137}Ba spectrum with respect to the zero-order ^{138}Ba levels. This reflects the isotope shift between the two isotopes already discussed in Ref. 6.

The singlet–triplet mixing coefficient β_{exp} resulting from the fit of the experimental hyperfine energies is given in Table 1. Tabulated are the 6*snh* $J = 5$ levels with dominant $^1H_5$ character and the corresponding triplet admixture coefficient β_{exp}. The error in β_{exp} is given in parentheses and accounts for one standard deviation. The energy dependence of β_{exp} turns out to be almost linear for $n > 9$. In analyzing the data it was assumed that the 6*snh* $J = 5$ level at the highest energy has the largest $^1H_5$ fraction in its wave function. This can not be deduced from hyperfine structure alone, as two solutions may be found that both reproduce the hyperfine structure. The assumption may not be true for $n = 9$, as each of the two 6*snh* $J = 5$ levels is perturbed by $5d4f$ levels. For this reason the two solutions for $n = 9$ are

Table 1. Experimental (β_{exp}) and Theoretical (β_{th}) Triplet Admixture Coefficient in the 6*snh* $^1H_5$ Wave Function[a]

n	$W(^1H_5)$ (cm^{-1})	β_{exp}	β_{th}	ΔW (MHz)	N
9	40 670.612	−.469 (1)	.367	3	12
	40 675.930	.406 (1)			
10	40 934.813	−.578 (1)	.602	4	7
11	41 125.524	−.599 (1)	.620	4	11
12	41 270.830	−.612 (1)	.631	5	11
13	41 383.941	−.622 (2)	.638	3	11
14	41 473.688	−.629 (2)	.643	4	12
16	41 605.327	−.643 (4)	.648	4	10
18	41 695.557	−.649 (7)	.651	3	10
20	41 760.080	−.66 (1)	.652	2	10
25	41 859.074	−.66 (2)	.653	3	11
30	41 912.827	−.64 (4)	.653	2	11
35	41 945.229	−.67 (2)	.653	4	11

[a] See Eqs. (2). In the last two columns the maximum difference ΔW (in megahertz) between experimental and fitted hyperfine energy and the number of hyperfine levels N used in the fitting are given.

Table 2. Fine-Structure Splitting of the 6*snh* Configuration[a]

	ΔW			
n	$J = 4$	$J = 6$	$J = 5$	$W(^3H_5)$
7				39 785.128
8	−4282 (5)[b]		−38 973 (200)	40 313.750
9	−9448 (5)[b]	132 508 (12000)	−159 445 (200)	40 675.930
10	−781 (5)[b]	15 346 (170)	25 234 (200)	40 933.971
11	−307 (9)	6 999 (18)	9 396 (5)[b]	41 125.211
12	−169 (9)	4 250 (12)	5 277 (5)[b]	41 270.654
13	−102 (9)	2 916 (11)	3 474 (5)[b]	41 383.825
14	−67 (9)	2 145 (11)	2 488 (5)[b]	41 473.605
16	−31 (9)	1 309 (11)	1 467 (5)[b]	41 605.278
18	−13 (10)	886 (11)	968 (5)[b]	41 695.525
20	−13 (6)	626 (8)	678 (5)[b]	41 760.057
25	−4 (9)	315 (9)	336 (5)[b]	41 859.063
30	−2 (9)	191 (9)	193 (5)[b]	41 912.821
35	0 (6)	121 (6)	120 (5)[b]	41 945.225
40	0 (6)	80 (6)	80 (5)[b]	41 966.251

[a] Differences $\Delta W(J) = W(J) - W(^3H_5)$ are given relative to the $^3H_5$ (or the $6snh_{9/2}$ $J = 5$) level (in megahertz). The error in parentheses is one standard deviation. The last column gives the absolute energy (in wavelengths) of the $^3H_5$ level.

[b] From direct measurement.

Table 3. Energies of the $5d4f$ Levels

$5d_{3/2}4f$	$J = 4$	39 747.0(3) cm^{-1}
	$J = 4$	39 835.3(3) cm^{-1}
	$J = 5$	39 888.1(3) cm^{-1}
	$J = 1$	39 893.48(7) cm^{-1} [a,b]
	$J = 2$	39 898.56(19) cm^{-1} [a,c]
$5d_{5/2}4f$	$J = 4$	40 501.9(3) cm^{-1}
	$J = 4$	40 614.3(3) cm^{-1} [c]
	$J = 6$	40 619(7) cm^{-1} [d]
	$J = 5$	40 650.5(3) cm^{-1}
	$J = 1$	40 662.86(18) cm^{-1} [a]
	$J = 2$	40 678.91(18) cm^{-1} [a,c]
	$J = 5$	40 733.819(6) cm^{-1}
	$J = 1$	40 736.81(15) cm^{-1} [a,b]
	$J = 2$	40 792.94(15) cm^{-1} [a,c]

[a] From Ref. 7.
[b] Strongly mixed with $6snp$.
[c] Tentative assignment.
[d] From MQDT; see Subsection 3.C.

included in Table 1. In analyzing $n = 10$ we were unable to fit the experimental data unless it was assumed that one of the two previously assigned $6snh$ $J = 5$ levels[6] actually is a $J = 4$ state. This observation led to a prediction of the position of the missing $J = 5$ level, which subsequently was found close to this predicted value. The same procedure resulted in the prediction and observation of the perturbed $6s9h$ $J = 5$ level. In the analysis of the $n = 9$ hyperfine-structure, the $5d4f$ admixture in the wave function of the zero-order basis could not be neglected. This admixture reduces the $6snh$ fraction significantly, thus affecting the hyperfine structure. In the fine-structure basis of the perturbed levels an extra term was added that merely served to reduce the $6snh$ fraction. The β parameter for the two $J = 5$ levels will then be slightly different.[5] Hyperfine structure related to the $5d4f$ fraction in the wave function is neglected in the calculation. In the fitting routine for $n = 9$ an admixture of 7% $5d4f$ $J = 5$ in the level labeled $6s9h\ ^1H_5$, 0.4% in $6s9h\ ^3H_5$, and 8% $5d4f$ $J = 6$ in $6s9h\ ^3H_6$ was deduced. In particular, the perturbation of the $6snh\ ^3H_6$ series may be inaccurately determined because, owing to the interaction with the single $5d4f$ $J = 6$ perturber, the $6s9h\ ^3H_6$ level is located 5 cm^{-1} away from the nearest observable $6s9h$ state, resulting in only weak hyperfine-induced effects.

In Table 2 the fine-structure splitting of the $6snh$ configurations as determined from direct (^{138}Ba) or indirect (hyperfine-structure) measurements is given with respect to the nearly unperturbed $6snh\ ^3H_5$ levels. The absolute energy of the $6snh\ ^3H_5$ state is determined from wavelength measurements.[6] For high-n values the $^3H_5$ energies are (within the experimental error) smoothed to reduce the scatter in the quantum defect (see Subsection 3.B). The grouping of the fine-structure levels, also shown in Fig. 2, indicates a jj-coupling scheme for the $6snh$ configuration. This is corroborated by the extracted triplet admixture in the level labeled $^1H_5$ as given in Table 1. In a pure jj-coupling scheme this level is labeled $6s_{1/2}nh_{11/2}$ and has a triplet admixture of $(5/11)^{1/2} = 0.674$ (from the jj–LS transformation matrix calculated in SL coupling[12]). Although the absolute value of the extracted singlet–triplet mixing agrees well with experiment, its sign does not. By using the ambiguity in the hyperfine-structure analysis, this disagreement can be solved in principle by reversing the assignment of the two $J = 5$ levels all over the series. This would, however, destroy the jj-coupling characteristic grouping of $6snh_{11/2}$ ($J = 5, 6$) and $6snh_{9/2}$ ($J = 4, 5$) levels (see Fig. 2). Although inverted fine structure has been demonstrated for nonpenetrating Rydberg states of alkalilike atomic systems,[13] the symmetry in the observed $6snh$ fine structure makes such inverted fine structure highly unlikely in the case of barium and is therefore discarded. A similar situation occurred, although less clearly, in the analysis of the $6sng$ hyperfine structure and is manifest there in the large value of the MQDT singlet–triplet mixing parameter θ_{12} of -0.90.[5] In the remaining part of this paper this sign controversy will be ignored, as it is not important in the further analysis.

$6snh$ $J = 4, 6$ level energies deduced from the hyperfine-structure analysis may be compared with published values of Zaki Ewiss *et al.*[14] and Lahaye *et al.*[15] Zaki Ewiss *et al.* observed $6s20h\ ^3H_4$ in direct excitation from the metastable $6s5d\ ^3D_3$ level, whereas Lahaye *et al.* observed $6s40h\ ^3H_6$ by using two-step excitation of $6s40g\ ^3G_5$ in a weak electric field. Both measurements are in excellent agreement with the present results.

B. Perturbers: General

From the level energies in Table 2, quantum defects with respect to the $6s$ ionization limit of the $6snh$ $J = 4, 5, 6$ series are calculated; they are plotted in Fig. 3 as a function of $\nu_{5d[5/2]}$ (Lu–Fano plot). Far away from $5d4f$ and $5d5f$ perturbers, the quantum defects of the four fine-structure levels show a linear energy dependence as expected from the Rydberg–Ritz formula for unperturbed series. Moreover, the two-by-two ordering typical for jj coupling is obvious. Owing to interaction with the $5d_{5/2}4f$ configuration located between $n = 8$ and $n = 10$ and with $5d_{3/2}4f$ states between $n = 6$ and $n = 8$, the quantum defects of the $6snh$ series vary strongly in this region. These perturbations are manifest more strongly in the $6snh_{11/2}$ ($J = 5, 6$) than in the $6snh_{9/2}$ ($J = 4, 5$) series. The $6snh$ series may be perturbed by eight levels of the $5d4f$ configuration: one $J = 6$ ($5d_{5/2}4f$), three $J = 5$ (two $5d_{5/2}4f$, one $5d_{3/2}4f$), and four $J = 4$ (two $5d_{5/2}4f$, two $5d_{3/2}4f$). These levels have been located directly ($J = 4, 5$) or indirectly ($J = 6$; see Subsection 3.C). In Table 3 we have collected the $5d4f$ level energies as determined in this study ($J = 4, 5, 6$) as well as values obtained by Armstrong *et al.*[7] ($J = 1, 2$). For $J = 0, 2, 3$ data are still missing. Table 3 clearly shows the subdivision of the $5d4f$ level energies into two groups: $5d_{3/2}4f$ between 39 700 and 39 900 cm^{-1} and $5d_{5/2}4f$ between 40 500 and 40 800 cm^{-1}.

C. Multichannel Quantum-Defect Theory Analyses

The $6snh$–$5d4f$ configuration interaction may be analyzed within the framework of the MQDT.[1,3] In the MQDT the complex interaction of several Rydberg series converging to different ionization limits is characterized by using a limited number of parameters related to the quantum defects and the matrix elements of the electrostatic interaction $1/r_{12}$ between the different series. The MQDT parameters are extracted from experimental data. With a complete set of parameters, level energies, wave functions, and autoionization widths of the individual members of the series may be determined.

In analyzing the $6snh$ Rydberg series with the MQDT an

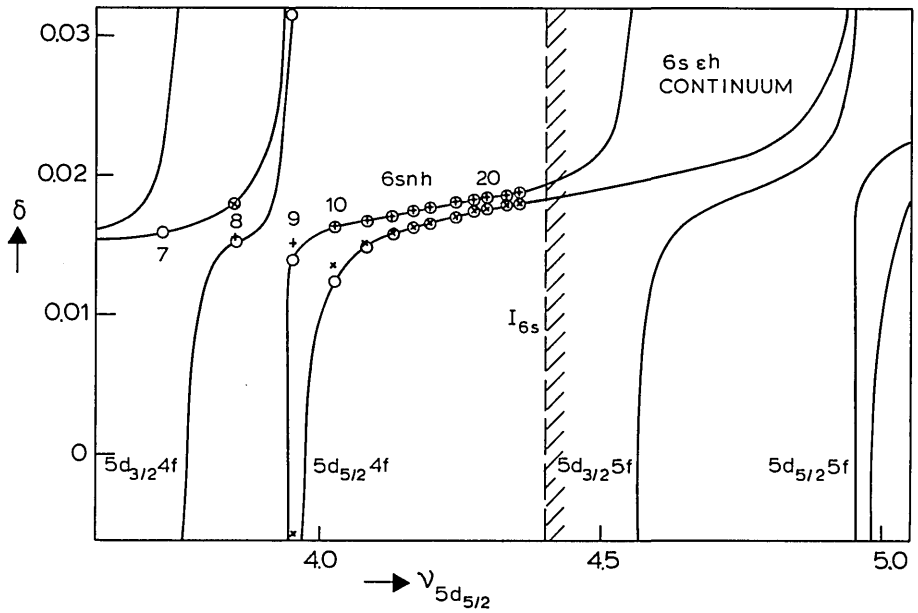

Fig. 3. Part of the Lu–Fano plot of the $6snh$ $J = 4, 5, 6$ Rydberg levels: +, $J = 4$; O, $J = 5$; ×, $J = 6$. For clarity only the $J = 5$ MQDT curves are plotted. Perturbing $5d4f$ and $5d5f$ levels (of $J = 5$) lie upon vertical branches of the plot.

approach different from the analyses of lower-l Rydberg series was chosen. The $6snp$, $6snd$, $6snf$, and $6sng$ series were analyzed in the close-coupling formulation of the MQDT.[1,3,5] Parameters of interest then are eigen quantum defects μ_α of the close-coupling channels, their energy dependence $d\mu_\alpha$, and a $U_{i\alpha}$ matrix representing the transformation between close-coupling channels α and collision channels i (jj coupled). In the original work of Fano and coworkers on photoabsorption by hydrogen[16] and later on xenon and argon[17] the close-coupling channels were LS coupled, which simplifies the analysis considerably. In barium significant deviations from LS coupling have been shown to occur,[1] complicating the analysis. Especially in the case of two interacting Rydberg series with nonpenetrating Rydberg electrons the close-coupling formalism leads to results that are difficult to interpret. Owing to the near equality of the quantum defects in the $6snh$ and $5dn'f$ Rydberg series (both close to zero) the close-coupling channels will be strongly mixed combinations of $6snh$ and $5dn'f$. The $U_{i\alpha}$ matrix, commonly generated from the jj–LS transformation matrix through successive small Eulerian rotation angles ($\theta_{i\alpha}$), is far from the jj–LS transformation matrix, and the eigen quantum defects μ_α differ considerably from the experimentally determined quantum defects δ_i.

An alternative way to parameterize the channel coupling in the MQDT was recently developed by Giusti-Suzor and Fano[18] and Cooke and Cromer.[19] In this shifted R-matrix formalism, parameters are easier to extract and directly related to physical quantities. Parameters here are the quantum defects δ_i (and their energy dependence $d\delta_i$) of the Rydberg series in the absence of channel coupling and the R-matrix elements R_{ij} [for N channels, only $N(N-1)/2$ matrix elements may be fitted independently; usually one chooses $R_{ii} = 0, R_{ij} = R_{ji}$]. R_{ij} is directly proportional to the configuration interaction matrix element between channels i and j. Above the ionization limit it is proportional to the square root of the autoionization linewidths.

As the $J = 4, 5, 6$ MQDT analyses have to be performed independently, the results are presented separately.

J = 6

In the case of the $6snh$–$5dn'f$ $J = 6$ series interaction, a simple two-channel analysis was performed. The two channels represent the $6snh_{11/2}$ Rydberg series converging to the $6s$ ionization limit at 42 034.90 cm^{-1} and the $5d_{5/2}nf_{7/2}$ series converging to the $5d_{5/2}$ limit at 47 709.73 cm^{-1}. In principle six parameters had to be fitted: two quantum defects δ_1 and δ_2, one R_{12}-matrix element, and their energy dependences $d\delta_1$, $d\delta_2$, and dR_{12}. As in this research the small-energy range below the $6s$ ionization limit containing not more than one level of each $5dn'f$ series (i.e., $n' = 4$) was studied, only information on the $5d4f$–$6snh$ configuration interaction could be extracted, and energy dependences dR and $d\delta$ involving $5dn'f$ channels were taken to be zero. From Fig. 3 a nonzero value for the energy dependence $d\delta_2$ of the $6snh$ channel is obvious. For $J = 6$ the four remaining parameters were highly accurately fitted to the $6snh$ $J = 6$ level energies deduced from hyperfine structure. The difference between experimental and fitted level energies, W_{th}–W_{exp}, did not exceed 0.01 cm^{-1}. With the parameters given in Table 4, unknown level energies and wave-function compositions were also calculated. For $6s8h$ and $5d4f$ ($J = 6$), level energies of 40 312.0(2) and 40 619(7) cm^{-1}, respectively, are predicted. The errors in the quoted energies are due merely to the inaccuracy in the $6s9h$ $J = 6$ level energy deduced from hyperfine structure. The $5d4f$ admixture in $6s9h$ $J = 6$ was calculated to be 8%, in good agreement with the value deduced from the hyperfine-structure analysis of $n = 9$ (Subsection 3.A).

J = 5

The number of channels required in the analysis of the $5dn'f$–$6snh$ $J = 5$ configuration interaction is five. In jj coupling these may be labeled $5d_{5/2}nf_{5/2}$, $5d_{5/2}nf_{7/2}$, $5d_{3/2}nf_{7/2}$;

$6snh_{11/2}$; and $6snh_{9/2}$ (channels 1, 2, 3, 4, and 5, respectively), converging, respectively, to the $5d_{5/2}$ (47 709.73 cm^{-1}), $5d_{3/2}$ (46 908.75 cm^{-1}), and $6s$ (42 034.90 cm^{-1}) limits. In this case five quantum defects δ_i, two (equal) energy dependences $d\delta_i$ for the $6s$ channels ($i = 4, 5$), and ten R_{ij} elements had to be determined. As in the case of the $J = 6$ series energy dependences for the $5dnf$ series were taken to be zero. However, only six R_{ij} elements can be extracted from $5d4f$ and $6snh$ level energies. The R_{12}, R_{13}, and R_{23} elements determine the $5d4f$ intermediate coupling and do not directly influence the $6snh$–$5dn'f$ channel mixing. Their values, however, may be deduced from the level energies of the $5dnf$ autoionizing series above the $6s$ limit. $5dnf$ $J = 4$, 5 levels were recently observed by us for $n = 5$–50.[12] A preliminary MQDT analysis of the $5d_{3/2}nf$ $J = 5$ series perturbed by two $5d_{5/2}n'f$ series gave energy-independent R-matrix elements and energy-dependent quantum defects. Extrapolation of these data to $n = 4$ provided starting values for the fit of the $6snh$ and $5d4f$ $J = 5$ level energies (R_{12}, R_{13}, and R_{23} constant; δ_1, δ_2, and δ_3 fitted). The R_{45} matrix element representing the $6snh$ $J = 5$ angular-momentum coupling cannot be extracted from level energies alone. However, the wave-function composition of the two $6snh$ $J = 5$ levels as a function of n deduced from hyperfine structure and given in Table 1 (β_{exp}) could be used for this purpose, as has been demonstrated in analyses of lower-l $6snl$ Rydberg series in barium,[1,5] using the close-coupling formulation of the MQDT. In the fitting procedure a starting value $R_{45} = 0$ was chosen, as the $6snh$ Rydberg series in the absence of configuration interaction is expected to be close to jj coupled. In an iterative procedure R_{45} was manually adjusted after each energy fit with the other parameters (five δ's, six R_{ij}'s, and one $d\delta$) by inspecting the calculated wave-function composition. It turned out that a good energy fit could be obtained with several combinations of the relevant R_{ij} elements. Only with the parameter set given in Table 4 was the n dependence of the singlet–triplet mixing coefficient β_{exp} also correctly accounted for. In this case only three R_{ij} elements turned out to be significant. Moreover, within the experimental error the quantum defects δ_4 and δ_5 of the $6snh$ channels were equal and took the same value as in the $J = 6$ case. With the eight parameters δ_1, δ_2, δ_3 (for $5d4f$ level energies), $\delta_4 = \delta_5$, $d\delta_4 = d\delta_5$ (for $6snh$ level energies far away from perturbers), R_{41} (for $5d_{5/2}4f$–$6snh_{11/2}$ configuration interaction), R_{52} (for $5d_{5/2}4f$–$6snh_{9/2}$ configuration interaction), and R_{53} (for $5d_{3/2}4f$–$6snh_{9/2}$ configuration interaction) with $R_{45} = -0.0015$ (for $6snh$ intermediate coupling), level energies were fitted to within 0.01 cm^{-1} for $n > 12$ and 0.09 cm^{-1} for $n = 8$–12, whereas for the wave-function composition the difference between the calculated and the experimental singlet–triplet mixing coefficient $\Delta\beta(n) = |\beta_{th}(n) - \beta_{exp}(n)|$ did not exceed the value 0.03 ($n = 9$–40) (see Table 1).

$J = 4$

In the $6snh$–$5d4f$ $J = 4$ MQDT analysis five channels have to be included: one $6snh$, two $5d_{3/2}nf$, and two $5d_{5/2}nf$ channels. For a correct MQDT analysis the four R-matrix elements between the $6snh$ $J = 4$ channel and the four $5dn'f$ channels have to be extracted. However, the limited set of experimental data does not permit such a procedure: four parameters to be extracted from two only slightly perturbed $6snh$ $J = 4$ levels (i.e., $n = 8$, 9). The only conclusion that could be drawn from the scarce data available is that the $5d_{5/2}4f$–$6snh$ $J = 4$ interaction is relatively weak (R-matrix elements smaller than 0.02). The $6snh$ $J = 4$ levels may be fitted with the same quantum defect as deduced for the $J = 5$ and 6 case. Further analysis of the $J = 4$ case may be performed in the autoionizing regime, where the $5dnf$–$6s\epsilon h$ R-matrix elements determine the linewidth of the $5d_{3/2}nf$ levels below the $5d_{3/2}$ limit (together with an additional $6s\epsilon f$ channel).

Inspection of the $J = 4$, 5, 6 data leads to the conclusion that the $6snh_{11/2}$ series interacts most strongly with $5d_{5/2}4f$, whereas for the $6snh_{9/2}$ series the interaction with $5d_{3/2}4f$ seems the most important. The near equality of the $6snh_{11/2}$ $J = 5$, 6 level energies and the $6snh_{9/2}$ $J = 4$, 5 level energies obviously is not a result of differences in quantum defect for $6snh_{11/2}$ and $6snh_{9/2}$ but merely reflects different configuration interaction with $5d4f$. For $J = 5$ this effect is most clearly visible when the $5d5f$ autoionizing levels are also added to the Lu–Fano plot, as shown in Fig. 3. The varying quantum defects for higher $6snh_{11/2}$ and $6snh_{9/2}$ $J = 5$ levels reflect a type of anticrossing between the $5d4f$ and $5d5f$ levels.

Table 4. MQDT Parameters

$J = 6$	$5d_{5/2}nf_{7/2}$	$6s_{1/2}nh_{11/2}$			
	$\delta_1 = 0.0649$	$\delta_2 = 0.0185$ $d\delta_2 = -0.17$			
	$R_{12} = 0.051$				
$J = 5$	$5d_{5/2}nf_{5/2}$	$5d_{5/2}nf_{7/2}$	$5d_{3/2}nf_{7/2}$	$6s_{1/2}nh_{11/2}$	$6s_{1/2}nh_{9/2}$
	$\delta_1 = 0.0412$	$\delta_2 = 0.0576$	$\delta_3 = 0.0387$	$\delta_4 = 0.0185$ $d\delta_4 = -0.17$	$\delta_5 = 0.0185$ $d\delta_5 = -0.17$
	$R_{12} = 0.02$				
	$R_{13} = 0.133$	$R_{23} = 0.056$			
	$R_{14} = 0.052$	$R_{24} = 0$	$R_{34} = 0$		
	$R_{15} = 0$	$R_{25} = -0.015$	$R_{35} = -0.038$	$R_{45} = -0.00015$	
$J = 4$	$6s_{1/2}nh_{9/2}$				
	$\delta = 0.0185$ $d\delta = -0.17$				

Although the observed $6snh$ fine-structure splitting is due primarily to configuration interaction with $5d4f$ and $5d5f$, the fine-structure splitting characteristic of jj coupling is visible at all observed n values (except $n = 9$, which nearly coincides with $5d_{5/2}4f$), including $n = 8$. This is reflected in the equivalence of the MQDT parameters for both the $6snh_{11/2}$–$5d_{5/2}n'f$ interaction for $J = 5$, 6 and the $6snh_{9/2}$–$5d_{5/2}n'f$ interaction for $J = 4$, 5; it probably also holds for the $5d_{3/2}n'f$–$6snh$ interactions, although this cannot be concluded unambiguously from the data.

4. CONCLUSIONS

Experimental hyperfine-structure splittings of the barium $6snh$ Ryberg series, perturbed by levels of the $5d4f$ configuration, can be reproduced accurately by diagonalization of the hyperfine-interaction Hamiltonian [Eq. (1)] in a fine-structure basis of the even isotopes, taking into account the mixing of the two $J = 5$ levels. For fine-structure states with a relatively small admixture of doubly excited $5d4f$ states only the $6snh$ fraction in their wave function is of importance.

The triplet admixture coefficient β in the fine-structure state labeled $6snh\ ^1H_5$ varies slowly (linearly) with energy for $n > 9$ and may be reproduced in a five-channel MQDT model including singlet–triplet mixing. The high value of β leads to the conclusion that the $6snh$ Rydberg series is best described in a jj-coupled representation. Despite the high value of the orbital angular momentum and the correspondingly small overlap with the ion core, the fine structure of the $6snh$ Rydberg series of barium is not due solely to the spin–orbit interactions of the nh electron, as in the corresponding case of helium. Effects of configuration interaction still have a major influence on the fine-structure splitting of the $l = 5$ Rydberg series of barium.

ACKNOWLEDGMENTS

The authors gratefully acknowledge financial support from the Netherlands Organisation for the Advancement of Research and the Foundation for Fundamental Research on Matter.

REFERENCES

1. M. Aymar, Phys. Rep. **110,** 163 (1984), and references therein.
2. W. Hogervorst, Comm. At. Mol. Phys. **13,** 69 (1983).
3. U. Fano and A. R. P. Rau, *Atomic Collisions and Spectra* (Academic, New York, 1986).
4. R. D. Cowan, *The Theory of Atomic Structure and Spectra* (U. California Press, Berkeley, Calif., 1981).
5. W. Vassen and W. Hogervorst, Z. Phys. D **8,** 149 (1988).
6. W. Vassen, E. A. J. M. Bente, and W. Hogervorst, J. Phys. B **20,** 2383 (1987).
7. J. A. Armstrong, J. J. Wynne, and P. Esherick, J. Opt. Soc. Am. **69,** 211 (1979).
8. E. A. J. M. Bente and W. Hogervorst, Phys. Rev. A **36,** 4081 (1987).
9. H. P. Palenius, Phys. Lett. **56A,** 451 (1976).
10. R. J. de Graaff, E. A. J. M. Bente, W. Hogervorst, and A. Wännström, Phys. Rev. A **37,** 4532 (1988).
11. C. E. Burkhardt, R. L. Corey, W. P. Garver, J. J. Leventhal, M. Allegrini, and L. Moi, Phys. Rev. A **34,** 80 (1986).
12. E. U. Condon and G. H. Shortley, *The Theory of Atomic Spectra* (Cambridge U. Press, Cambridge, 1967).
13. J. Detrich and A. W. Weiss, Phys. Rev. A **25,** 1203 (1982).
14. M. A. Zaki Ewiss, W. Hogervorst, W. Vassen, B. H. Post, and H. Wijnen, Z. Phys. A **322,** 385 (1985). The $6s20h$ level at 41 760.06 cm^{-1} reported in this paper has erroneously been assigned as $6s20h\ ^3H_6$.
15. C. T. W. Lahaye, W. Hogervorst, and W. Vassen, Z. Phys. D **7,** 37 (1987).
16. U. Fano, Phys. Rev. A **2,** 353 (1970).
17. K. T. Lu, Phys. Rev. A **4,** 579 (1971); and C. M. Lee and K. T. Lu, Phys. Rev. A **8,** 1241 (1973).
18. A. Giusti-Suzor and U. Fano, J. Phys. B **17,** 215 (1984).
19. W. E. Cooke and C. L. Cromer, Phys. Rev. A **32,** 2725 (1985).